JOURNAL OF AGRICULTURAL AND FOOD CHEMISTRY

Article

pubs.acs.org/JAFC

(−)-Epigallocatechin Gallate Induces Fas/CD95-Mediated Apoptosis through Inhibiting Constitutive and IL-6-Induced JAK/STAT3 Signaling in Head and Neck Squamous Cell Carcinoma Cells

Hui-Yi Lin,[†] Shin-Chen Hou,[‡] Shi-Chen Chen,[†] Ming-Ching Kao,[‡] Chien-Chih Yu,[†] Shinji Funayama,[§] Chi-Tang Ho,[∥] and Tzong-Der Way*[,‡,⊥]

[†]School of Pharmacy, College of Medicine, College of Pharmacy, and [‡]Department of Biological Science and Technology, College of Life Sciences, China Medical University, Taichung, Taiwan

[§]Department of Kampo Pharmaceutical Sciences, Nihon Pharmaceutical University, 10281 Komuro, Inamachi, Saitama 362-0806, Japan

[∥]Department of Food Science, Rutgers University, New Brunswick, New Jersey, United States

[⊥]Institute of Biochemistry, College of Life Science, National Chung Hsing University, Taichung, Taiwan

Supporting Information

ABSTRACT: In this study, we examined the effects of several plant-derived natural compounds on head and neck squamous cell carcinoma (HNSCC) cells. The results revealed that (−)-epigallocatechin gallate (EGCG) demonstrated the most efficient cytotoxic effects on HNSCC cells. We then investigated the underlying molecular mechanism for the potent proapoptotic effect of EGCG on HNSCC. Cell apoptosis was observed in the EGCG-treated SAS and Cal-27 cells in a time- and dose-dependent manner. In concert with the caspase-8 activation by EGCG, an enhanced expression in functional Fas/CD95 was identified. Consistent with the increased Fas/CD95 expression, a drastic decrease in the Tyr705 phosphorylation of STAT3, a known negative regulator of Fas/CD95 transcription, was shown within 15 min in the EGCG-treated cells, leading to downregulation of the target gene products of STAT3, such as bcl-2, vascular endothelial growth factor (VEGF), mcl-1, and cyclin D1. An overexpression in STAT3 led to resistance to EGCG, suggesting that STAT3 was a critical target of EGCG. Besides inhibiting constitutive expression, EGCG also abrogated the interleukin-6 (IL-6)-induced JAK/STAT3 signaling and further inhibited IL-6-induced proliferation on HNSCC cells. In comparison with apigenin, curcumin, and AG490, EGCG was a more effective inhibitor of IL-6-induced proliferation on HNSCC cells. Overall, our results strongly suggest that EGCG induces Fas/CD95-mediated apoptosis through inhibiting constitutive and IL-6-induced JAK/STAT3 signaling. This mechanism may be partially responsible for EGCG's ability to suppress proliferation of HNSCC cells. These findings provide that EGCG may be useful in the chemoprevention and/or treatment of HNSCC.

KEYWORDS: *EGCG, Fas/CD95, IL-6, STAT3, HNSCC*

INTRODUCTION

Head and neck squamous cell carcinoma (HNSCC) is a global malignancy and affects 600,000 people worldwide annually, including 42,000 people in the United States.[1,2] The addiction to betel, tobacco, and alcohol is found to be highly correlated with the risk of HNSCC.[3−5] Although this disease is highly curable during its early stage, more than half of oral cancer patients progress to advanced stages.[6] Today, the overall prognosis of late stage HNSCC patients is still dismal. However, there have been very few studies on this subject related to HNSCC, and yet studies in this area might lead to new approaches in the prevention and treatment of this important group of human cancers.

STAT3, which is believed to be associated with transforming growth factor (TGF)-β and epidermal growth factor receptor (EGFR) signaling, is constitutively activated in many human cancers.[8−11] Its transcriptional activation seems to be regulated by phosphorylation at the Ser727 residue, apparently via mitogen-activated protein kinase (MAPK) or a mammalian target of rapamycin (mTOR) pathways.[12,13] Over 90% of head and neck cancers show constitutively activated STAT3.[7] Moreover, inhibition of STAT3 function leads to growth inhibition of HNSCC.[14−16] This evidence supports that STAT3 is an important molecular target for HNSCC therapy. Although tyrosine kinase receptors such as EGFR are capable of inducing STAT3 phosphorylation, the reported incidence of active EGFR pathway in HNSCC varies significantly. Thus, it is possible that additional mechanisms participate in the constitutive activation of STAT3 in this malignancy. IL-6, a cytokine mostly involved in the modulation of immunoresponse and inflammatory response, also has a role in the regulation of apoptosis, proliferation, angiogenesis, and differentiation.[17,18] A previous study identified IL-6 as a major secretory ligand stimulating STAT3 activation by HNSCC.[19] When IL-6 bound to cell surface cytokine receptors such as JAK family

Received: October 25, 2011
Revised: February 7, 2012
Accepted: February 7, 2012
Published: February 7, 2012

dx.doi.org/10.1021/jf204362n | J. Agric. Food Chem. 2012, 60, 2480−2489

Table 1. IC_{50} Values of Natural Compounds on HNSCC Cells after 24 h Treatment[a]

	IC_{50}										
cell lines	EGCG	TF1	TF2	TF3	5GG	apigenin	rutin	emodin	osthole	geniposide	magnonol
SAS	6.26	14.71	14.04	10.24	16.28	>40	>40	>40	3.9	>40	>40
Cal-27	16.15	29.67	31.24	27.63	>40	>40	>40	>40	>40	>40	>40
Ca9-22	18.1	37.46	39.45	>40	>40	>40	>40	>40	>40	>40	>40

[a]Cells were treated with natural extract compounds for 24 h and examined for cell viability by MTT assay. Data were obtained from three separate experiments.

protein kinases, inactive cytoplasmic STAT3 was phosphorylated at the Tyr705 residue and underwent dimerization, thus permitting its translocation into the nucleus and inducing transcription of specific target genes.[20] Some of these genes were involved in cell survival (Bcl-2 and Bcl-xL) and cell growth (cyclin D1). Expression of a dominant-negative STAT3 in HNSCC cells inhibited proliferation, cyclin D1 promoter activity, and cellular levels of cyclin D1 mRNA and protein. The levels of the antiapoptotic Bcl-2 and Bcl-xL proteins were also diminished.[21] Thus, development of pharmacologically safe and effective therapeutic agents that can block constitutive or inducible activation of STAT3 will be beneficial to the treatment of HNSCC.

Plant-derived natural products have gained considerable attention in recent years as cancer chemopreventive agents. In the past two decades, numerous chemopreventive constituents have been isolated and/or synthesized and evaluated for their efficacy in a variety of biological assays. EGCG is the major polyphenol component of green tea and a potential anticarcinogenic factor.[22] In this study, we examined the effect of several plant-derived natural compounds on HNSCC cells. We found that EGCG showed the most clearly cytotoxic effects. EGCG induced cell apoptosis via the expression of Fas/CD95 in SAS and Cal-27 cells. Consistent with the increased Fas/CD95 expression, EGCG inhibited STAT3 phosphorylation and translocation to the nucleus. The downstream proteins of STAT3 also decreased. We also showed that EGCG could block the activation of IL-6 on JAK/STAT3 signaling. The findings of the present study could make EGCG a potentially effective chemopreventive and therapeutic natural product on head and neck squamous cell cancer.

MATERIALS AND METHODS

Materials. TF-1, TF-2, and TF-3 were extracted from black tea and separated by chromatography on a LH-20 column to a purity of >99%, as described previously.[23] 5GG was isolated from the leaves of *Macaranga tanarins* (L.) as described previously.[24] Osthole, apigenin, EGCG, rutin, emodin, geniposide, magnolol, curcumin, propidium iodide (PI), and annexin V were purchased from Sigma-Aldrich (St. Louis, MO). Stocks of natural compounds in DMSO were prepared fresh as required and then diluted 1000× with the relevant cell culture medium to the required final concentrations. IL-6 was purchased from Santa Cruz Biotechnology (Santa Cruz, CA). The caspase inhibitor Z-VAD-FMK was obtained from Promega Corporation (Madison, WI). Antibodies and reagents were purchased from commercial sources: JAK-1, JAK-2, PhosphoTyr$^{1022/1023}$-JAK1, Phospho Tyr$^{1007/1008}$-JAK2, STAT3, PhosphoSer^{727}-STAT3, p21, poly(ADP)ribose polymerase (PARP), Bcl-2, cleaved caspase-3, and caspase-8 were obtained from Cell Signaling Technology, Inc. (Beverly, MA); PhosphorTyr^{705}-STAT3, VEGF, p53, p73, and Mcl-1 were obtained from Santa Cruz Biotechnology; Fas/CD95 and cyclin D1 were from BD Biosciences (Franklin Lakes, NJ); anti-β-actin, horseradish peroxidase-conjugated anti-rabbit IgG, anti-mouse IgG, and enhanced chemiluminescence (ECL) reagents were purchased from Sigma-Aldrich. Cell culture materials were obtained from Invitrogen (Burlington, Ontario, Canada).

Cell Culture. Cal-27 (CRL-2095) cells were purchased from the American Type Culture Collection (Manassas, VA). SAS (JCRB0260) and Ca9-22 (JCRB0625) cells were obtained from the Japanese Collection of Research Bioresources (Tokyo, Japan). SAS and CAL 27 were cultured in Dulbecoo's modified Eagle's medium (DMEM) containing 10% fetal bovine serum and 1% penicillin−streptomycin. Ca9-22 was cultured in MEM containing 10% fetal bovine serum and 1% penicillin−streptomycin. These cells were maintained at 37 °C in a humidified atmosphere at 95% air and 5% CO_2.

Cell Viability. Cells (1×10^4) were seeded on the 24-well cell culture cluster overnight, then treated with different concentrations of compounds and incubated for 24 h. Next, 40 μL of MTT (3-(4, 5-dimethylthiazol-2-yl)-2,5-diphenyltetrazolium bromide) (stock concentration 2 mg/mL, Sigma Chemical Co.) was added to each well; the volume of each well was 500 μL; then the culture was incubated for 2 h at 37 °C. The MTT-formazan crystals were formed, and then 250 μL of DMSO was added to dissolve the crystals. Finally, the absorbance at OD 590 nm was detected by the enzyme-linked immunosorbent assay (ELISA) reader.

Flow Cytometry. The cell cycle analysis was determined by flow cytometry. Cells were cultured in 60 mm Petri dishes and incubated for various times. After being trypsinized and washed twice with ice-cold PBS, the cells were fixed with 70% ice-cold ethanol overnight at −20 °C. After centrifugation, the cell pellets were treated by RNAase A, exposed to PI, and then analyzed by flow cytometry (FACScan, BD Biosciences, Mountain View, CA). The percentage was analyzed by Cell Quest software (BD Biosciences).

Western Blotting. The cells (1×10^6) were seeded onto a 100 mm tissue culture dish in 10% FBS medium and cultured for 24 h. The cells were then incubated in 10% FBS medium treating with various doses of EGCG for various time periods. Cells were washed three times with PBS and then lysed in gold lysis buffer (10% glycerol, 1% Triton X-100, 137 mM NaCl, 10 mM NaF, 1 mM EGTA, 5 mM EDTA, 1 mM sodium pyrophosphate, 20 mM Tris-HCl, pH 7.9, 100 mM β-glycerophosphate, 1 mM sodium orthovanadate, 0.1% SDS, 10 μg/mL aprotinin, 1 mM phenylmethylsulfonyl fluoride, and 10 μg/mL leupeptin). Protein content was determined against a standardized control, using the Bio-Rad protein assay kit (Bio-Rad Laboratories). A total of 50 μg of protein was separated by SDS−PAGE and transferred to nitrocellulose filter paper (Schleicher & Schuell, Inc., Keene, NH). Nonspecific binding on the nitrocellulose filter paper was minimized with a blocking buffer containing nonfat dry milk (5%) and Tween 20 (0.1%, v/v) in PBS (PBS/Tween 20). Then the filter paper was incubated with primary antibodies followed by incubation with horseradish peroxidase-conjugated goat anti-mouse antibody (1:2500 dilution, Roche Applied Science, Indianapolis, IN). Expression levels of actin, STAT3, phosphor-STAT3 were detected by enhanced chemiluminescence (ECL, Amersham, Arlington Heights, IL).

RNA Extraction and Quantitative Real-Time PCR. Total RNA was isolated from SAS cells using the RNeasy system according to the instructions of the manufacturer. RNA quantification was done using spectrophotometry. Quantitative real-time PCR was performed by the StepOnePlus real-time PCR system (Applied Biosystems) with the preset PCR program, and GAPDH (glyceraldehyde 3-phosphate dehydrogenase) was applied as an internal control. The sequences (5′−3′) for the primer pairs of Fas/CD95 and GAPDH, respectively, were as follows: Fas/CD95, CAAGGGATTGAAATTGAGGA

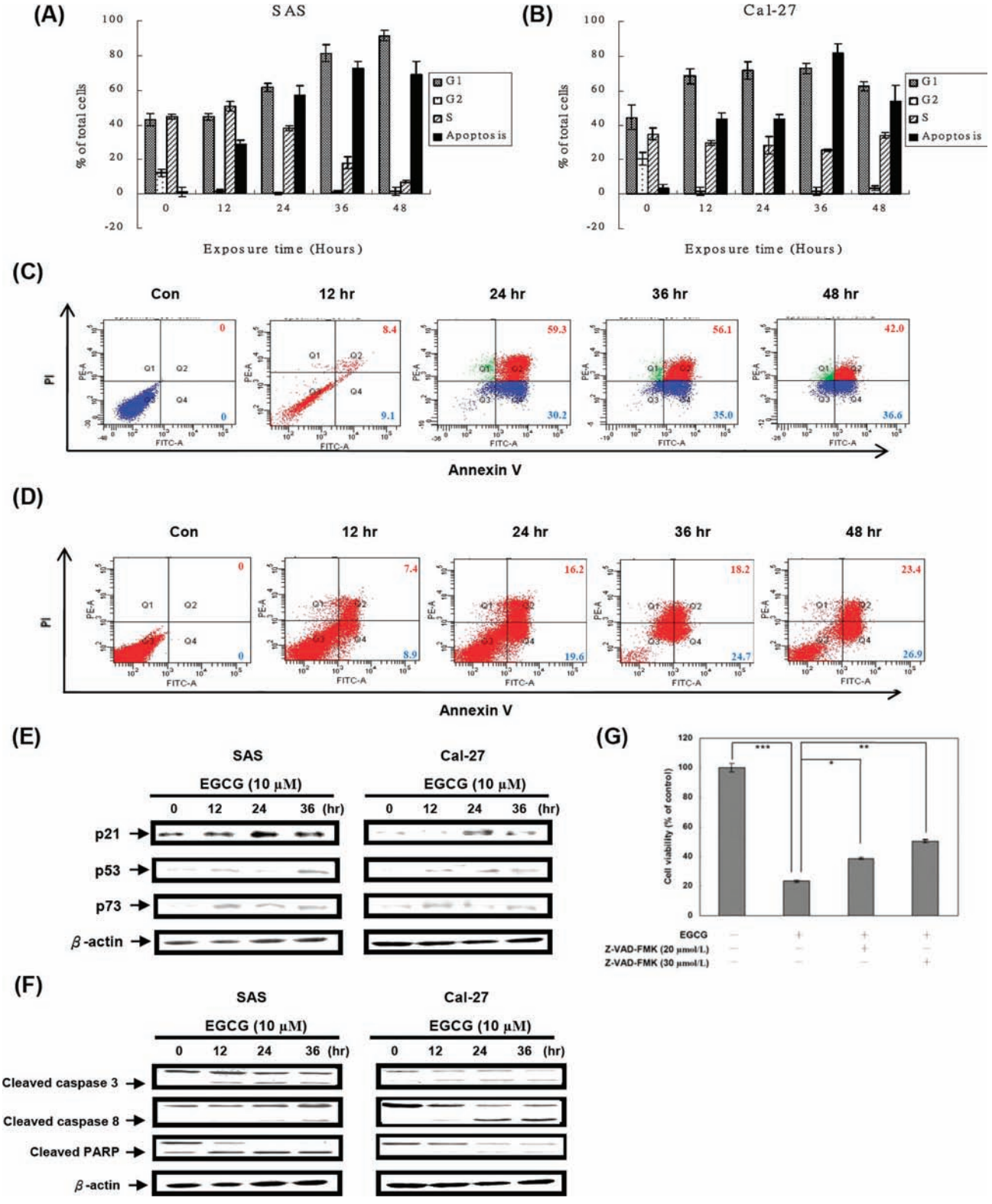

Figure 1. The proliferation-inhibitory effect of EGCG on HNSCC cells. The time effect of EGCG on cell cycle distribution: SAS (A) and Cal-27 (B) cells were treated with 10 μM EGCG for 12, 24, 36, and 48 h and analyzed for propidium iodide stained DNA content by flow cytometry. The indicated percentages are the mean of three independent experiments, each in duplicate. The apoptotic fraction of SAS (C) and Cal-27 (D) cells detected by annexin V staining (*x*-axis)/propidium iodide (*y*-axis) staining after different treatments. The lower right quadrant of the plot indicates early apoptotic cells that are only positive for annexin V. Results are representative of three independent experiments. (E) SAS and Cal-27 cells were treated with vehicle (DMSO) and EGCG (10 μM) for the indicated time. Cells were then harvested and lysed for the detection of p21, p53, p73, and β-actin protein expression. (F) SAS and Cal-27 cells were treated with vehicle (DMSO) and EGCG (10 μM) for the indicated time. Cells were then harvested and lysed for the detection of cleavages in caspase-3, caspase-8, PARP, and β-actin protein expression. Western blot data presented are representative of those obtained in at least three separate experiments. (G) Z-VAD-FMK or the vehicle (DMSO) was added to the medium at 1 h before the 10 μM EGCG treatment. After the 24 h incubation, the SAS cell viability was determined using MTT assay. This experiment was repeated three times. Bars represent the SD.

dx.doi.org/10.1021/jf204362n | J. Agric. Food Chem. 2012, 60, 2480−2489

(forward), and GACAAAGCCACCCCAAGTTA (reverse); GAPDH, GTCAACGGATTTGGTCGTATT (forward), and AGTCTTCTGGGTGGCAGTGAT (reverse).

Confocal Microscopy. After treatment, cells were fixed with methanol, blocked with 3% bovine serum albumin, stained with anti-β-tubulin monoclonal antibody, and then treated with FITC-conjugated anti-mouse IgG antibody. Nuclear staining was done with 4,6-diamidino-2-phenylindole (DAPI). Cells were imaged with Leica TCS SP2 spectral confocal system.

Transient Transfections. The SAS cells were transiently transfected with FLAG-tagged expression vectors encoding a dominant active STAT3 (CA-STAT3). The CA-STAT3 vector was a kind gift from Dr. Mien-Chie Hung. One day before transfection, cells were seeded in a 6-well plate without antibiotics with the density of 30 to 40%. For plasmid transfections, 2 μg of plasmid DNA was premixed with lipofectamine 2000 (Invitrogen, Carlsbad, CA) in Opti-MEM and added to wells for 6 h.

Statistics. All values were expressed as mean ± SD. Each value is the mean of at least three separate experiments in each group. The results were subjected to the one-way ANOVA test using GraphPad Prism software. Asterisks indicate that the values are significantly different from the control (*, $P < 0.05$; **, $P < 0.01$; ***, $P < 0.001$).

RESULTS

Effect of Natural Compounds on HNSCC Cell. There are numerous cancer preventive compounds present in natural products. To evaluate preventive effects against HNSCC, we treated three HNSCC cell lines, namely, SAS, Cal-27, and Ca9-22, with eleven natural compounds. The HNSCC cells were treated with the eleven natural compounds for 24 h and examined for cell viability by MTT assay (Figure S1 in the Supporting Information). As shown in Table 1, HNSCC cell proliferation could be inhibited significantly by treatment with tea polyphenols, such as EGCG, TF-1, TF-2, and TF-3. Among these tea polyphenols, EGCG was the most effective one in our assay. These results may provide a rationale for the potential use of EGCG as chemopreventive agent for HNSCC patients.

EGCG Inhibited HNSCC Cell Proliferation and Induced Apoptosis. To determine whether EGCG altered cell cycle progression on HNSCC cells, we performed flow cytometry by using PI stain. Both SAS and Cal-27 cells were treated with 10 μM EGCG and then harvested at 12, 24, 36, and 48 h. After 12 h EGCG treatment, both SAS (Figure 1A) and Cal-27 (Figure 1B) cell cycles were arrested in G_1 phase, resulting in cell apoptosis in a time-dependent manner. We further checked whether EGCG caused apoptosis. Apoptosis was detected in cells treated with EGCG in a time-dependent manner, as measured by FACS analysis using annexin V/PI staining. In the presence of EGCG (10 μM), a significantly elevated number of apoptotic cells were detected in SAS (Figure 1C) and Cal-27 (Figure 1D) cells. Moreover, we examined the expression of G1 related cell cycle control proteins and apoptosis related proteins on Western blot analysis. SAS and Cal-27 cells were treated with 10 μM EGCG for indicated durations, and 50 μg of each whole-cell extract was used for Western blot analyses. After 12 h treatment with EGCG, both SAS and Cal-27 cells showed increased level of p53, p21, and p73 proteins (Figure 1E). Moreover, an apparent cell apoptosis was observed in SAS and Cal-27 cells at the dosage of 10 μM EGCG within 12 h, showing cleavage patterns of caspase-8, caspase-3, and PARP in immunoblotting (Figure 1F). Consistent with this finding, the caspase inhibitor Z-VAD-FMK significantly inhibited the EGCG-induced apoptosis in a dose-dependent manner (Figure 1G).

Involvement of Fas/CD95 in EGCG-Induced Apoptosis. Because caspase-8 was activated by EGCG, we examined the expression level of caspase-8-associated death receptors, such as Fas/CD95.[25] Indeed, an apparent increase in Fas/CD95 expression was found in the EGCG-treated SAS and Cal-27 cells (Figure 2A), suggesting a significant involvement of

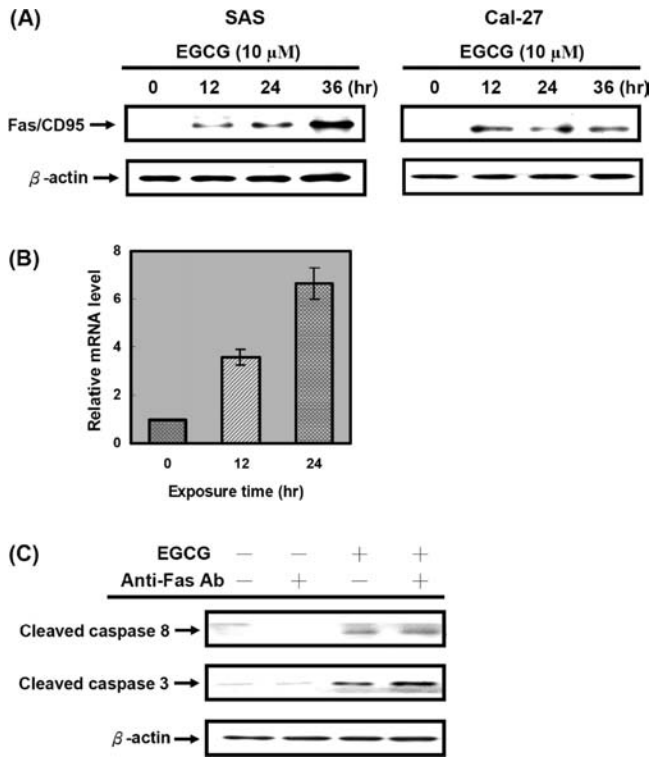

Figure 2. Immunoblot analysis for the expression levels of Fas/CD95. (A) SAS and Cal-27 cells were treated with vehicle (DMSO) or EGCG (10 μM) for the indicated time. Cells were then harvested and lysed for the detection of Fas/CD95 and β-actin protein expression. (B) SAS cells were treated with vehicle (DMSO) or EGCG (10 μM) for the indicated time, and mRNA of Fas/CD95 and GAPDH was determined. Quantitative real-time PCR was performed by the StepOnePlus real-time PCR system, and GAPDH was applied as an internal control. Data were plotted by mean ± SD ($n = 3$). The value of control was set to 1. (C) After incubation with 10 μM EGCG for 12 h, the agonistic anti-Fas/CD95 antibody (clone CH-11; dilution, 1:5,000) was added into the culture medium for the SAS cells. After treatment with the antibody for 4 h, the cells were then prepared for immunoblot analyses of cleaved caspase-8 and cleaved caspase-3.

Fas/CD95 in the EGCG-induced apoptosis. To confirm whether the increased expression in Fas/CD95 was due to its transcriptional induction, we performed quantitative real-time PCR analysis for Fas/CD95 mRNA. The EGCG-treated SAS cells clearly showed an increased expression in Fas/CD95 mRNA (Figure 2B). Then, we examined whether this upregulated Fas/CD95 was functional in inducing apoptotic signals. We stimulated the EGCG-treated cells by an apoptosis inducing anti-Fas/CD95 antibody (clone CH-11) and found that the pretreated cells became more sensitive to this antibody (Figure 2C). This indicated that the newly synthesized Fas/CD95 was functional in mediating the apoptotic signals in the EGCG-treated HNSCC cells.

Decrease in the Expression Level of Phosphorylated STAT3s. Transcription of Fas/CD95 is negatively regulated by

STAT3, especially by its phosphorylated forms Tyr705-phosphorylated STAT3 and Ser727-phosphorylated STAT3.[26] Thus, the increase in the expression level of Fas/CD95 by the EGCG treatment in this study encouraged us to investigate a possible decrease in the expression level of the phosphorylated STAT3s. Indeed, the expression level of Tyr705-phosphorylated STAT3, a major phosphorylated STAT3, was drastically decreased in a dose- and time-dependent manner, although that of total STAT3 was mostly unchanged (Figures 3A, 3B). In contrast to the rapid decrease in the Tyr705-phosphorylated

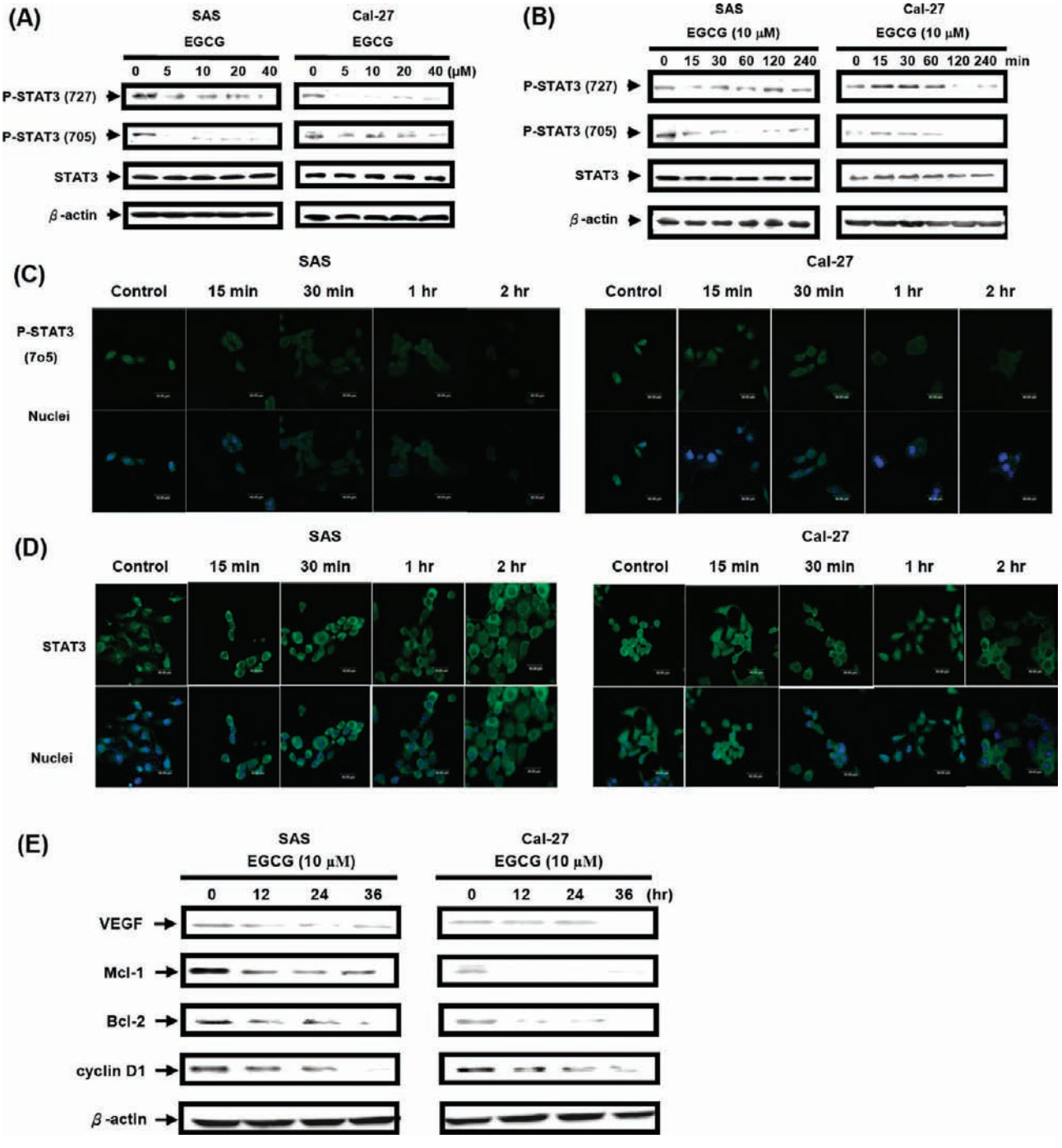

Figure 3. EGCG inhibits STAT3 phosphorylation. SAS and Cal-27 cells were treated with vehicle (DMSO) or EGCG (5, 10, 20, and 40 μM) at 37 °C for 1 h (A) or EGCG (10 μM) at 37 °C for various times (B). Immunoblotting was used to measure levels of Ser727-phosphorylated [P-STAT3 (727)], Tyr705-phosphorylated STAT3 [P-STAT3 (705)] and total STAT3. Western blot data presented are representative of those obtained in at least three separate experiments. (C) SAS and Cal-27 cells were treated with vehicle (DMSO) or EGCG (10 μM) for indicated durations. The active Tyr705-phosphorylated STAT3 is confirmed to be in the nuclei (green signal). (D) SAS and Cal-27 cells were treated with vehicle (DMSO) or EGCG (10 μM) for indicated durations, and then analyzed for the distribution of STAT3 by immunocytochemistry using a confocal laser scanning microscope. (E) To assess the expression levels in the downstream gene products of STAT3, such as VEGF, Mcl-1, Bcl-2, and cyclin D1, the immunoblot analysis was done using the SAS and Cal-27 cells exposed to EGCG (10 μM) for indicated durations. Western blot data presented are representative of those obtained in at least three separate experiments.

dx.doi.org/10.1021/jf204362n | J. Agric. Food Chem. 2012, 60, 2480–2489

STAT3 expression level, a gradual decrease was found in the expression level of Ser727-phosphorylated STAT3 (Figure 3B). To ensure that this effect of EGCG was specific on the phosphorylated STAT3s, changes in the expression levels of phosphorylated STAT1 were examined using immunoblot analysis, resulting in no change in the phosphorylated STAT1 expression (data not shown). Under resting conditions, and in the nonphosphorylated state, STAT3 is retained in the cytoplasm. It translocates to the nucleus when phosphorylated. Phosphorylation induces STAT3 dimerization, thus permitting its translocation into the nucleus. To confirm that EGCG suppresses nuclear translocation of phosphorylated STAT3, HNSCC cells were grown on a glass slide and were treated with either EGCG or vehicle alone, immunostained with antibody to Tyr705-phosphorylated STAT3. Figure 3C clearly demonstrates that EGCG prevented the translocation of the Tyr705-phosphorylated STAT3 to the nucleus in SAS and Cal-27 cells, consistent with the EGCG-induced inhibition of STAT3 phosphorylation. Whether EGCG modulates the nuclear localization of STAT3 was examined by using nonphosphorylated STAT3 antibody. These results indicate that STAT3 is present in the nucleus of SAS and Cal-27 and that EGCG-treatment suppresses the nuclear presence of STAT3 (Figure 3D).

Downregulation in the STAT3 Target Genes. Several individual targets of STAT3 have been identified, including bcl-2, VEGF, mcl-1, and cyclin D1, reflecting the role of STAT3 in promoting survival and cell cycle progression.[10] To determine the expression level in the downstream gene products of STAT3, we investigated the expression levels of the protein products of these genes by immunoblot assay. All of the gene products were found to be decreased in their expression level by the EGCG treatment (Figure 3E). The downregulation in these genes suggested a profound antitumor potential of EGCG even in vivo.

STAT3 Overexpression Leads to Resistance to EGCG-Induced Apoptosis. If STAT3 was a critical target of EGCG, overexpression of STAT3 should attenuate EGCG-induced apoptosis. To assess this hypothesis, we did a STAT3-overexpression experiment using cDNA of CA-STAT3 (a constitutively active mutant dimerized by cysteine−cysteine bridges instead of pTyr-SH2 interaction). Despite EGCG treatment, the STAT3-overexpressing SAS cells had a clearly detectable level in the expression of Tyr705-phosphorylated STAT3, which was fragile against EGCG in our system (Figure 4A). As a result, the EGCG-treated STAT3-overexpressing cells showed no enhanced cleavages in PARP and no decreased in the expression level of cyclin D1, in comparison with the controls including the empty vector-transfected cells (Figure 4B). Moreover, the EGCG-treated STAT3-overexpressing cells showed significantly reduced number of apoptotic cells, in comparison with the control cells (Figure 4C). These data suggested that EGCG might target, at least in part, STAT3 in the HNSCC cells.

EGCG Inhibits IL-6-Inducible STAT3 Phosphorylation in HNSCC Cells. In a recent report, IL-6 was identified as a major secretory ligand stimulating STAT3 activation by acting on the gp130 coreceptor in an autocrine/paracrine fashion in HNSCC.[19] Because IL-6 is a growth factor for HNSCC and induces Tyr705-phosphorylated STAT3, we checked whether EGCG could inhibit IL-6-induced Tyr705-phosphorylated STAT3. SAS and Cal-27 cells were incubated with EGCG for different times and examined for IL-6-inducible Tyr705-

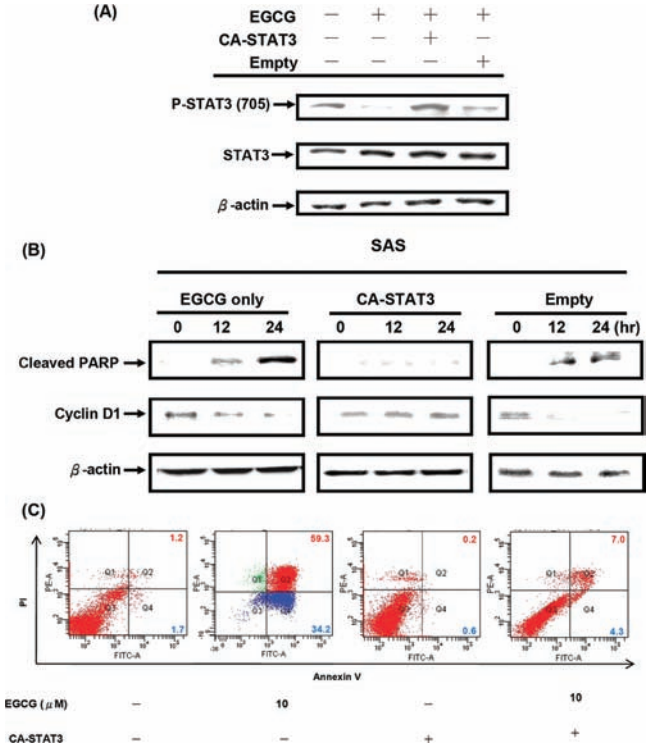

Figure 4. Resistance to the EGCG-induced apoptosis in the STAT3-overexpressing HNSCC cells. (A) SAS cells were transfected with CA-STAT3 or empty vector. Twenty-four hours after transfection, cells were treated with 10 μM EGCG for 1 h. After harvesting, cells were lysed and prepared for Western blotting analysis using antibodies against P-STAT3 (705) and total STAT3. β-Actin is shown as a loading control. (B) SAS cells were transfected with CA-STAT3 or empty vector. Twenty-four hours after transfection, cells were treated with 10 μM EGCG for indicated durations. Levels of cleaved PARP and cyclin D1 were examined in whole-cell extracts by Western blotting. Western blot data presented are representative of those obtained in at least three separate experiments. (C) SAS cells were transfected with CA-STAT3. Twenty-four hours after transfection, cells were treated with 10 μM EGCG for 24 h. The apoptotic fraction of cells detected by annexin V staining (x-axis)/propidium iodide (y-axis) staining after different treatments. The lower right quadrant of the plot indicates early apoptotic cells that are only positive for annexin V. Results are representative of three independent experiments.

phosphorylated STAT3. As seen in Figure 5A, IL-6-induced Tyr705-phosphorylated STAT3 was blocked by EGCG in a time-dependent manner. Exposure of cells to EGCG for 4 h was sufficient to completely suppress IL-6-induced Tyr705-phosphorylated STAT3. To confirm whether IL-6 could induce proliferation of HNSCC cells, SAS and Cal-27 cells were serum-starved for 12 h and then cultured in the absence or presence of IL-6 for 24 h. We next determined whether EGCG suppresses the proliferative effects of IL-6. MTT methods showed that IL-6-induced proliferation of SAS and Cal-27 cells was completely inhibited by EGCG (Figure 5B). We also compared EGCG to other inhibitors of STAT3 phosphorylation including curcumin, apigenin, and AG490 on their ability to inhibit the IL-6-induced proliferation. As shown in Figure 5C, EGCG was more potent than AG490, a well-characterized JAK2 inhibitor, and other inhibitors in suppressing the proliferation. These results coincide with their relative effects on STAT3 phosphorylation.

dx.doi.org/10.1021/jf204362n | J. Agric. Food Chem. 2012, 60, 2480−2489

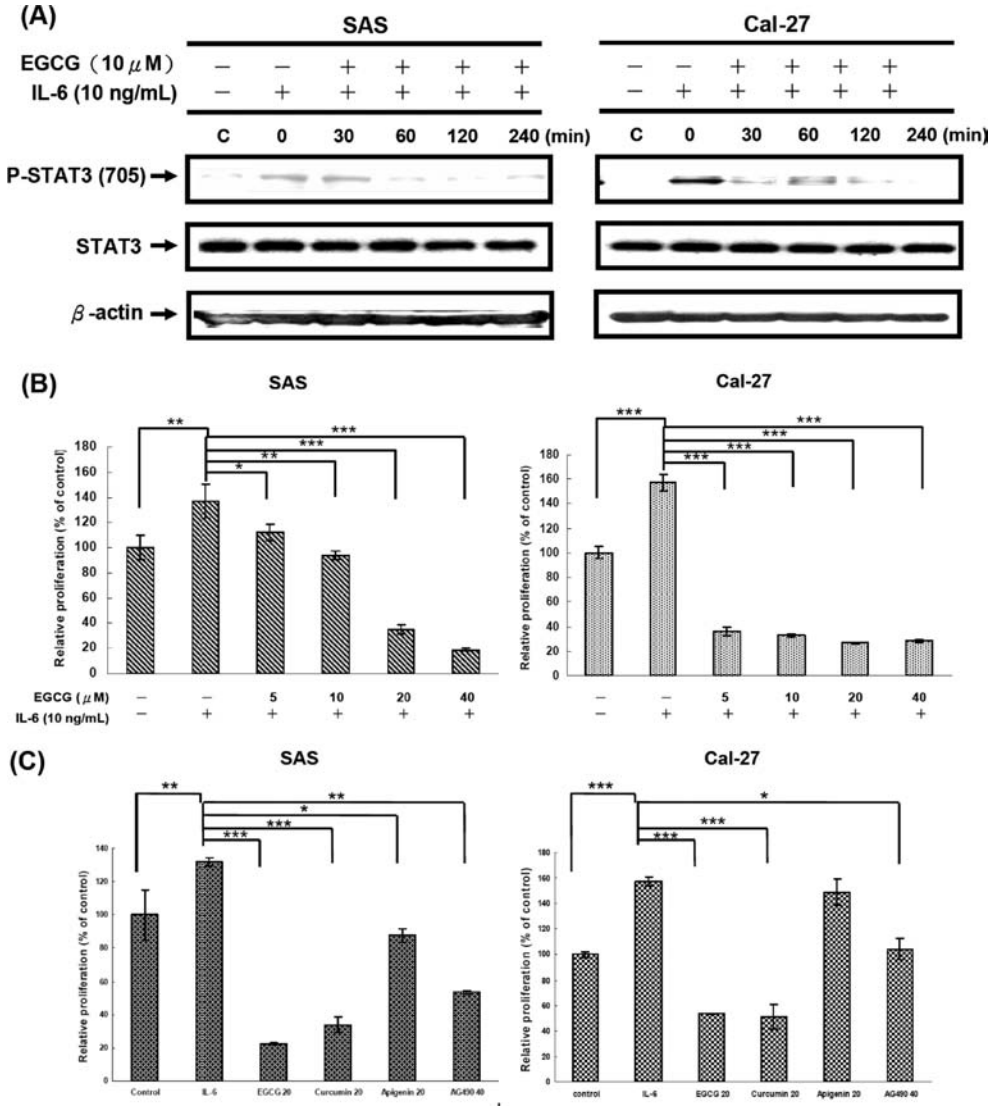

Figure 5. EGCG suppresses IL-6 induced STAT3 phosphorylation in human HNSCC cells. (A) SAS and Cal-27 cells were treated with 10 μM EGCG for indicated durations and stimulated with IL-6 (10 ng/mL) for 10 min. Levels of P-STAT3 (705) and total STAT3 were examined in whole-cell extracts by Western blotting. Western blot data presented are representative of those obtained in at least three separate experiments. (B) SAS and Cal-27 cells were serum starved for 12 h and then cultured with IL-6 (10 ng/mL) in the absence or presence of EGCG (5, 10, 20, and 40 μM) for 24 h in a serum-free medium. (C) SAS and Cal-27 cells cells were serum starved for 12 h and then cultured with IL-6 (10 ng/mL) in the absence or presence of EGCG (10 μM), curcumin (20 μM), apigenin (20 μM), and AG490 (40 μM) for 24 h in a serum-free medium. The cell viability was determined using MTT assay. This experiment was repeated three times. Bars represent the SD.

EGCG Inhibits IL-6-Inducible JAK1/2 Phosphorylation in HNSCC Cells. We have shown that EGCG may block IL-6-induced translocation of STAT3. To investigate whether the apoptosis induced by EGCG resulted from blocking of IL-6-induced JAK-STAT3 signaling pathway, SAS and Cal-27 cells were then incubated with EGCG for different times and examined for IL-6-inducible phosphorylation of JAK1/2. The phosphorylation of JAK1/2 was analyzed by Western blotting. As seen in Figure 6, IL-6-induced phosphorylation of JAK1/2 was blocked by EGCG in a time-dependent manner. Exposure of cells to EGCG for 4 h was sufficient to completely suppress IL-6-induced phosphorylation of JAK1/2. Our results suggest a new mechanism showing EGCG can inhibit the IL-6-induced JAK/STAT3 signaling in HNSCC cells and provide a potential drug for clinical cancer chemoprevention and/or treatment in the future.

DISCUSSION

We have presented that EGCG induces a significant concentration-dependent growth inhibition, causing G1 arrest of the cell cycle leading to cell apoptosis in human HNSCC cells. Our results are consistent with previous studies indicating that EGCG inhibited growth and induced apoptosis in human prostate, lung, colon, and gastric carcinoma and human leukemia cancer cell lines.[26−30] The EGCG concentrations used in the latter studies varied considerably. Our present study showed that HNSCC cells were very sensitive to the inhibitory effects of EGCG by comparing with cells from other human malignancies.

Among several proposed mechanisms for EGCG-induced apoptosis, the death receptor-associated mechanism has recently received much attention.[31] Siddiqui et al. first showed that EGCG sensitized TRAIL-resistant LNCaP cells to

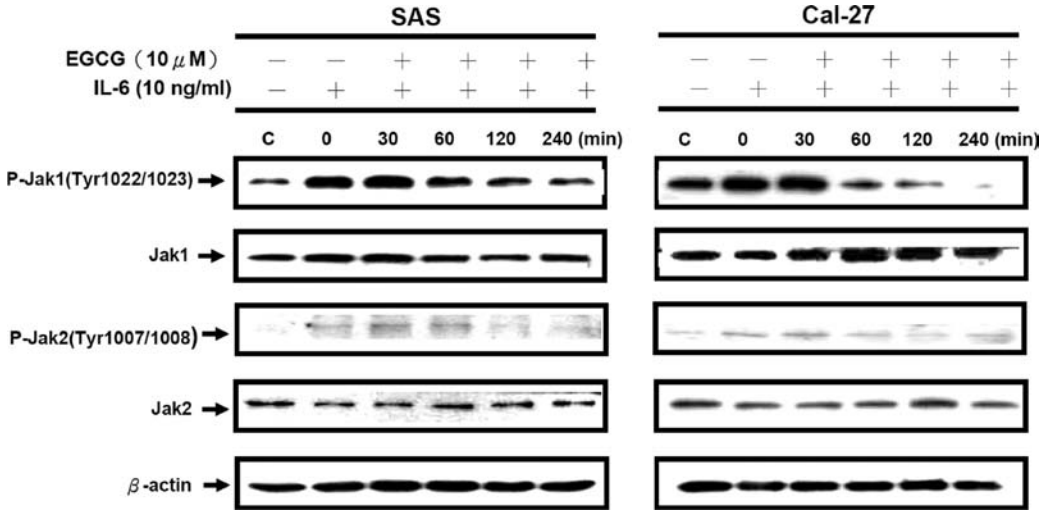

Figure 6. EGCG suppresses IL-6 induced JAK1/2 phosphorylation in human HNSCC cells. SAS and Cal-27 cells were treated with 10 μM EGCG for indicated durations and stimulated with IL-6 (10 ng/mL) for 10 min. Levels of P-JAK1 (Tyr1022/1023), P-JAK2 (Tyr1007/1008), and total JAK1 and JAK2 were examined in whole-cell extracts by Western blotting. Western blot data presented are representative of those obtained in at least three separate experiments.

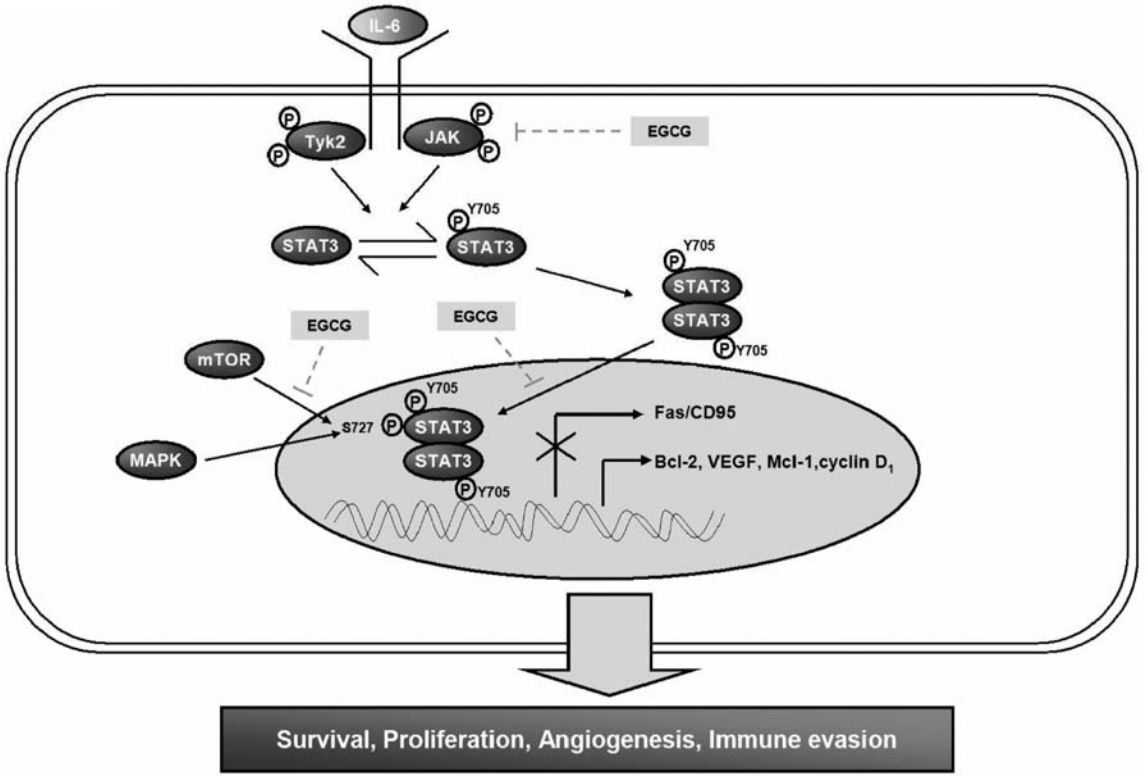

Figure 7. A schematic summary for the anticancer mechanisms of EGCG shown in the present study. This inactivation of JAK/STAT3 by EGCG may lead to the abrogation of the STAT3-mediated cancer properties, including survival, proliferation angiogenesis, and immune evasion, and increase sensitivity to apoptosis through upregulation of Fas/CD95.

TRAIL-mediated apoptosis through modulation of intrinsic and extrinsic apoptotic pathways. When combined with EGCG, Apo2L/TRAIL exhibited enhanced apoptotic activity in LNCaP cells characterized by three major molecular events.[31] These findings strongly suggested a critical involvement of the upregulated death receptor superfamily mediated signals in EGCG-induced cancer cell apoptosis. Furthermore, in this study, upregulation in another death receptor Fas/CD95 was first identified in EGCG-treated HNSCC cells, resulting in enhanced apoptosis via caspase 8 activation. However, it remains to be elucidated whether the death receptor-mediated apoptotic mechanism is ubiquitous in the EGCG-induced apoptosis in malignant cells.

It has been shown that transcription of Fas/CD95 was suppressed by the transcription factor STAT3.[24] An important downstream effect of STAT3 activation is the STAT3-dependent regulation of several antiapoptotic genes including Bcl-XL, survivin, and Mcl-1. These survival-promoting genes are highly

expressed in human cancers, especially in high-grade tumors.[32] Targeting STAT3 is thus considered to be a promising anticancer strategy and has actually been shown to be valid in inducing a significant cancer cell apoptosis. Furthermore, ablation of STAT3 expression in vivo has provided a deep insight into a new candidate approach for the treatment of human lymphoma.[33] In this context, our concerns converged in the potential effect of EGCG to downregulate STAT3 expression as a putative mechanism for increased Fas/CD95 expression. Indeed, we found a drastic decrease in the expression level of Tyr705-phosphorylated STAT3, a major active form of STAT3. Consistent with this finding, we confirmed the immediate disappearance in Tyr705-phosphorylated STAT3 from nuclei, where the activated STAT3 worked, in the EGCG-treated HNSCC cells by immunocytochemistry analysis. Nuclear translocation of activated STAT3 is a crucial event for its transcriptional function. Here, we reported that EGCG treatment suppressed the nuclear translocation of STAT3. If this striking downregulation in active STAT3 is substantially responsible for the EGCG-induced apoptosis through augmenting Fas/CD95 expression, then enforced expression of STAT3 in HNSCC cells should result in EGCG resistance. Indeed, the transfected cells clearly expressed Tyr705-phosphorylated STAT3 despite exposure to cytocidal concentrations of EGCG, resulting in less cell apoptosis. This finding strongly supports the concept that EGCG may induce apoptosis in HNSCC cells by targeting the oncogenic transcription factor STAT3.

HNSCC modulates the cytokine secretion profile of tumor infiltrating cells to escape from efficient immune responses and trigger its own malignant progression. It is hypothesized that these tumor cells develop mechanisms to evade the growth inhibitory effects of cytokines that are present in the tumor microenvironment. Various studies have shown significant alterations in signal transduction pathways engaged by cytokines that are associated with loss of growth inhibition in HNSCC. HNSCC cell lines are shown to secrete IL-6.[34] Additionally, IL-6 was detected at higher concentrations in the serum of patients with oral squamous cell carcinoma compared with sex and age-matched disease-free subjects.[35] The tissues of oral cancer patients with lymph node metastasis exhibited increased expression levels of IL-6 transcripts.[36] Moreover, IL-6 secreted by oral cancer cells plays a significant role in bone invasion,[37] and it has also been linked with radioresistance of HNSCC patients.[38] The constitutive activation of STAT3 in HNSCC has been shown to be mediated by the autocrine/paracrine stimulation of the IL-6, and this confers both proliferative and survival potential in this malignancy. To our knowledge, this is the first time to show that EGCG could abrogate IL-6-induced phosphorylation of STAT3 (Figure 7). Additionally, our previous studies have shown that EGCG had no effect on the phosphorylation status of STAT1. Regarding the inhibition effect on HNSCC cell proliferation, EGCG showed the most effective suppressive activity among other natural compounds (e.g., curcumin and apigenin) or synthetic molecules (e.g., AG 490). Furthermore, among the natural compounds mentioned in this study, EGCG was demonstrated to be the agent with the most potential to inhibit IL-6-induced proliferation of HNSCC cells. These consequences may be due to the suppression of EGCG on STAT3 signal transduction in vitro.

In conclusion, EGCG is a nontoxic natural compound and may be administered for a relatively long period of time without adverse side effects. With the ability to inhibit IL-6 signaling and block proliferation of HNSCC cells, combined with the well-established pharmacological safety, EGCG may be used as a potential therapeutic or chemopreventive agent for HNSCC patients.

■ ASSOCIATED CONTENT

Supporting Information

Figure depicting the proliferation-inhibitory effect of natural compounds on HNSCC cells. This material is available free of charge via the Internet at http://pubs.acs.org.

■ AUTHOR INFORMATION

Corresponding Author

*Department of Biological Science and Technology, College of Life Sciences, China Medical University, No.91 Hsueh-Shih Road, Taichung, Taiwan 40402, R.O.C. Tel: (886)-4-2205-3366 ext 2509. Fax: (886)-4-2207-0465. E-mail: tdway@mail.cmu.edu.tw.

Funding

This work was supported by Grant CMU98-P-06, and CMU99-COL-29-1 from the China Medical University of Taiwan.

Notes

The authors declare no competing financial interest.

■ ABBREVIATIONS USED

DMEM, Dulbecco's modified Eagle's medium; DMSO, dimethyl sulfoxide; EGFR, epidermal growth factor receptor; EGCG, (−)-epigallocatechin gallate; emodin, 1,3,8-trihydroxy-6-methylanthraquinone; 5GG, penta-*O*-galloyl-β-D-glucose; HNSCC, head and neck squamous cell carcinoma; IL-6, interleukin-6; MAPK, mitogen-activated protein kinase; MTT, 3-(4,5-dimethylthiazol-2-yl)-2,5-diphenyltetrazolium bromide; m-TOR, mammalian target of rapamycin; PCR, polymerase chain reaction; STAT3, signal transducer and activator of transcription 3; TF-1, theaflavin; TF-2a, theaflavin-3-gallate; TF-2b, theaflavin-3′-gallate; TF-3, theaflavin-3,3′-digallate; TGF-β, transforming growth factor-β; VEGF, vascular endothelial growth factor

■ REFERENCES

(1) Mignogna, M. D.; Fedele, S.; Lo Russo, L. The World Cancer Report and the burden of oral cancer. *Eur. J. Cancer Prev.* **2004**, *13*, 139−142.

(2) Jemal, A.; Siegel, R.; Xu, J.; Ward, E. Cancer statistics, 2010. *CA—Cancer J. Clin.* **2010**, *60*, 277−300.

(3) Weber, S. M.; Bornstein, S.; Li, Y.; Malkoski, S. P.; Wang, D.; Rustgi, A. K.; Kulesz-Martin, M. F.; Wang, X. J.; Lu, S. L. Tobacco-specific carcinogen nitrosamine 4-(methylnitrosamino)-1-(3-pyridyl)-1-butanone induces AKT activation in head and neck epithelia. *Int. J. Oncol.* **2011**, *39*, 1193−1198.

(4) Dhooge, I. J.; De Vos, M.; Van Cauwenberge, P. B. Multiple primary malignant tumors in patients with head and neck cancer: results of a prospective study and future perspectives. *Laryngoscope* **1998**, *108*, 250−256.

(5) Yen, A. M.; Chen, S. C.; Chen, T. H. Dose-response relationships of oral habits associated with the risk of oral pre-malignant lesions among men who chew betel quid. *Oral. Oncol.* **2007**, *43*, 634−638.

(6) Vokes, E. E.; Weichselbaum, R. R.; Lippman, S. M.; Hong, W. K. Head and neck cancer. *N. Engl. J. Med.* **1993**, *328*, 184−194.

(7) Nagpal, J. K.; Mishra, R.; Das, B. R. Activation of Stat-3 as one of the early events in tobacco chewing-mediated oral carcinogenesis. *Cancer* **2002**, *94*, 2393−2400.

(8) Lavecchia, A.; Di Giovanni, C.; Novellino, E. STAT-3 inhibitors: state of the art and new horizons for cancer treatment. *Curr. Med. Chem.* **2011**, *18*, 2359−2375.
(9) Bowman, T.; Garcia, R.; Turkson, J.; Jove, R. STATs in oncogenesis. *Oncogene* **2000**, *19*, 2474−2488.
(10) Yu, H.; Jove, R. The STATs of cancer—new molecular targets come of age. *Nat. Rev. Cancer* **2004**, *4*, 97−105.
(11) Darnell, J. E. Validating Stat3 in cancer therapy. *Nat. Med.* **2005**, *11*, 595−596.
(12) Wen, Z.; Zhong, Z.; Darnell, J. E. Jr. Maximal activation of transcription by Stat1 and Stat3 requires both tyrosine and serine phosphorylation. *Cell* **1995**, *82*, 241−250.
(13) Yokogami, K.; Wakisaka, S.; Avruch, J.; Reeves, S. A. Serine phosphorylation and maximal activation of STAT3 during CNTF signaling is mediated by the rapamycin target mTOR. *Curr. Biol.* **2000**, *10*, 47−50.
(14) Grandis, J. R.; Drenning, S. D.; Chakraborty, A.; Zhou, M. Y.; Zeng, Q.; Pitt, A. S.; Tweardy, D. J. Requirement of Stat3 but not Stat1 activation for epidermal growth factor receptor-mediated cell growth in vitro. *J. Clin. Invest.* **1998**, *102*, 1385−1392.
(15) Grandis, J. R.; Drenning, S. D.; Zeng, Q.; Watkins, S. C.; Melhem, M. F.; Endo, S.; Johnson, D. E.; Huang, L.; He, Y.; Kim, J. D. Constitutive activation of Stat3 signaling abrogates apoptosis in squamous cell carcinogenesis in vivo. *Proc. Natl. Acad. Sci. U.S.A.* **2000**, *97*, 4227−4232.
(16) Rubin Grandis, J.; Zeng, Q.; Drenning, S. D. Epidermal growth factor receptor-mediated Stat3 signaling blocks apoptosis in head and neck cancer. *Laryngoscope* **2000**, *110*, 868−874.
(17) Cavarretta, I. T.; Neuwirt, H.; Untergasser, G.; Moser, P. L.; Zaki, M. H.; Steiner, H.; Rumpold, H.; Fuchs, D.; Hobisch, A.; Nemeth, J. A.; Culig, Z. The antiapoptotic effect of IL-6 autocrine loop in a cellular model of advanced prostate cancer is mediated by Mcl-1. *Oncogene* **2007**, *26*, 2822−2832.
(18) Akira, S.; Taga, T.; Kishimoto, T. Interleukin-6 in biology and medicine. *Adv. Immunol.* **1993**, *54*, 1−78.
(19) Sriuranpong, V.; Park, J. I.; Amornphimoltham, P.; Patel, V.; Nelkin, B. D.; Gutkind, J. S. Epidermal growth factor receptor-independent constitutive activation of STAT3 in head and neck squamous cell carcinoma is mediated by the autocrine/paracrine stimulation of the interleukin 6/gp130 cytokine system. *Cancer Res.* **2003**, *63*, 2948−2956.
(20) Darnell, J. E. Jr.; Kerr, I. M.; Stark, G. R. Jak-STAT pathways and transcriptional activation in response to IFNs and other extracellular signaling proteins. *Science* **1994**, *264*, 1415−1421.
(21) Masuda, M.; Suzui, M.; Yasumatu, R.; Nakashima, T.; Kuratomi, Y.; Azuma, K.; Tomita, K.; Komiyama, S.; Weinstein, I. B. Constitutive activation of signal transducers and activators of transcription 3 correlates with cyclin D1 overexpression and may provide a novel prognostic marker in head and neck squamous cell carcinoma. *Cancer Res.* **2002**, *62*, 3351−3355.
(22) Lin, J. K.; Liang, Y. C. Cancer chemoprevention by tea polyphenols. *Proc. Natl. Sci. Counc., Repub. China, Part B: Life Sci.* **2000**, *24*, 1−13.
(23) Menet, M. C.; Sang, S.; Yang, C. S.; Ho, C. T.; Rosen, R. T. Analysis of theaflavins and thearubigins from black tea extract by MALDI-TOF mass spectrometry. *J. Agric. Food Chem.* **2004**, *52*, 2455−2461.
(24) Yokozawa, T.; Chung, H. Y.; Oura, H.; Nonaka, G.; Nishioka, I. Isolation of a renal function-facilitating constituent from the Oriental drug, salviae miltiorrhizae radix. *Nippon Jinzo Gakkaishi* **1989**, *31*, 1091−1098.
(25) Ivanov, V. N.; Bhoumik, A.; Krasilnikov, M.; Raz, R.; Owen-Schaub, L. B.; Levy, D.; Horvath, C. M.; Ronai, Z. Cooperation between STAT3 and c-jun suppresses Fas/CD95 transcription. *Mol. Cell* **2001**, *7*, 517−528.
(26) Onoda, C.; Kuribayashi, K.; Nirasawa, S.; Tsuji, N.; Tanaka, M.; Kobayashi, D.; Watanabe, N. (−)-Epigallocatechin-3-gallate induces apoptosis in gastric cancer cell lines by down-regulating survivin expression. *Int. J. Oncol.* **2011**, *38*, 1403−1408.
(27) Amin, A. R.; Wang, D.; Zhang, H.; Peng, S.; Shin, H. J.; Brandes, J. C.; Tighiouart, M.; Khuri, F. R.; Chen, Z. G.; Shin, D. M. Enhanced anti-tumor activity by the combination of the natural compounds (−)-epigallocatechin-3-gallate and luteolin: potential role of p53. *J. Biol. Chem.* **2010**, *285*, 34557−34565.
(28) Luo, K. L.; Luo, J. H.; Yu, Y. P. (−)-Epigallocatechin-3-gallate induces Du145 prostate cancer cell death via downregulation of inhibitor of DNA binding 2, a dominant negative helix-loop-helix protein. *Cancer Sci.* **2010**, *101*, 707−712.
(29) Yang, G. Y.; Liao, J.; Kim, K.; Yurkow, E. J.; Yang, C. S. Inhibition of growth and induction of apoptosis in human cancer cell lines by tea polyphenols. *Carcinogenesis* **1998**, *19*, 611−616.
(30) Britschgi, A.; Simon, H. U.; Tobler, A.; Fey, M. F.; Tschan, M. P. Epigallocatechin-3-gallate induces cell death in acute myeloid leukaemia cells and supports all-trans retinoic acid-induced neutrophil differentiation via death-associated protein kinase 2. *Br. J. Haematol.* **2010**, *149*, 55−64.
(31) Siddiqui, I. A.; Malik, A.; Adhami, V. M.; Asim, M.; Hafeez, B. B.; Sarfaraz, S.; Mukhtar, H. Green tea polyphenol EGCG sensitizes human prostate carcinoma LNCaP cells to TRAIL-mediated apoptosis and synergistically inhibits biomarkers associated with angiogenesis and metastasis. *Oncogene* **2008**, *27*, 2055−2063.
(32) Gritsko, T.; Williams, A.; Turkson, J.; Kaneko, S.; Bowman, T.; Huang, M.; Nam, S.; Eweis, I.; Diaz, N.; Sullivan, D.; Yoder, S.; Enkemann, S.; Eschrich, S.; Lee, J. H.; Beam, C. A.; Cheng, J.; Minton, S.; Muro-Cacho, C. A.; Jove, R. Persistent activation of stat3 signaling induces survivin gene expression and confers resistance to apoptosis in human breastca ncer cells. *Clin. Cancer Res.* **2006**, *12*, 11−19.
(33) Chiarle, R.; Simmons, W. J.; Cai, H.; Dhall, G.; Zamo, A.; Raz, R.; Karras, J. G.; Levy, D. E.; Inghirami, G. Stat3 is required for ALK-mediated lymphomagenesis and provides a possible therapeutic target. *Nat. Med.* **2005**, *11*, 623−629.
(34) Woods, K. V.; El-Naggar, A.; Clayman, G. L.; Grimm, E. A. Variable expression of cytokines in human head and neck squamous cell carcinoma cell lines and consistent expression in surgical specimens. *Cancer Res.* **1998**, *58*, 3132−3141.
(35) St John, M. A.; Li, Y.; Zhou, X.; Denny, P.; Ho, C. M.; Montemagno, C.; Shi, W.; Qi, F.; Wu, B.; Sinha, U.; Jordan, R.; Wolinsky, L.; Park, N. H.; Liu, H.; Abemayor, E.; Wong, D. T. Interleukin 6 and interleukin 8 as potential biomarkers for oral cavity and oropharyngeal squamous cell carcinoma. *Arch. Otolaryngol., Head Neck Surg.* **2004**, *130*, 929−935.
(36) Nagata, M.; Fujita, H.; Ida, H.; Hoshina, H.; Inoue, T.; Seki, Y.; Ohnishi, M.; Ohyama, T.; Shingaki, S.; Kaji, M.; Saku, T.; Takagi, R. Identification of potential biomarkers of lymph node metastasis in oral squamous cell carcinoma by cDNA microarray analysis. *Int. J. Cancer* **2003**, *106*, 683−689.
(37) Okamoto, M.; Hiura, K.; Ohe, G.; Ohba, Y.; Terai, K.; Oshikawa, T.; Furuichi, S.; Nishikawa, H.; Moriyama, K.; Yoshida, H.; Sato, M. Mechanism for bone invasion of oral cancer cells mediated by interleukin-6 in vitro and in vivo. *Cancer* **2000**, *89*, 1966−1975.
(38) De Schutter, H.; Landuyt, W.; Verbeken, E.; Goethals, L.; Hermans, R.; Nuyts, S. The prognostic value of the hypoxia markers CA IX and GLUT 1 and the cytokines VEGF and IL 6 in head and neck squamous cell carcinoma treated by radiotherapy 1/2 chemotherapy. *BMC Cancer* **2005**, *5*, 42.